Nuclear-state engineering in tripod systems using x-ray laser pulses

B. Nedaee-Shakarab, M. Saadati-Niari,* and F. Zolfagharpour
Department of Physics, Faculty of Sciences, University of Mohaghegh Ardabili, P.O. Box 179, Ardabil, Iran
(Received 30 May 2017; revised manuscript received 20 September 2017; published 24 October 2017)

Coherent superposition of nuclear states in tripod systems using three x-ray laser pulses is investigated theoretically. The laser pulses transfer the population from one ground state to an arbitrary superposition of other ground states using coincident pulses and stimulated Raman adiabatic passage techniques. The short wavelengths needed in the frame of the nuclei are achieved by envisaging an accelerated nucleus interacting with three x-ray laser pulses. This study exploits the Morris-shore transformation to reduce the tripod system into a coupled three-state Λ-like system and a noncoupled state. We calculated the required laser intensities which satisfy the conditions of coincident pulses and adiabatic passage techniques. Considering the spontaneous emission from excited state $|4\rangle$ and unstable ground states ($|2\rangle$, $|3\rangle$) to other states, we have used a master equation for numerical study, and the final fidelity of desired states with respect to the tolerance of laser intensities is studied numerically.

DOI: 10.1103/PhysRevC.96.044619

I. INTRODUCTION

In recent years, among the growing x-ray free electron laser (XFEL) [1] community worldwide, nuclear coherent population transfer (NCPT) with XFEL has received great attention [2–12]. Bürvenich *et al.* [2] have studied the interaction of XFEL with two-level nuclear systems theoretically. In their method [2], the gap between x-ray frequency and nuclear transition energy has been compensated by combining moderately accelerated target nuclei and novel x-ray lasers. The proposed scheme in [2] has been extended by Liao *et al.* [13,14] to three-level Λ-like nuclear systems in which two π pulses [15,16] and stimulated Raman adiabatic passage (STIRAP) [17–21] have been used respectively for nuclei with long and short lifetime excited states. Recently in Ref. [22] NCPT in the three level Λ-like systems was implemented by a train of coincident pulses [23–27]. In the coincident pulse technique the robustness of the system against the small variation of laser intensities and spontaneous emission rise by increasing the number of pulse pairs. In the limit of large number of coincident pulses, the technique of coincident pulses converges to the piecewise adiabatic passage (PAP) technique [28–30].

The four-state system in which three of the ground states are linked, by three separate fields, to a single excited state (tripod system) has become a popular system in quantum physics [31]. It has been shown that arbitrary one-qubit rotation gates can be implemented much more efficiently in tripod systems [32]. In recent years population transfer in tripod systems has been implemented using π-pulse and STIRAP techniques [25,31,33–35].

Unlike the case of atom-laser interaction, coherent control of nuclear states in tripod systems remains unchallenged. Coherent superposition of states in nuclear systems can be used in nuclear interferometry and nuclear spectroscopy. In the present paper, we introduce a nuclear tripod linkage pattern and investigate coherent superposition of states in this system. In our method, the short wavelengths needed in the frame of the nuclei are achieved by using an accelerated nuclear beam, interacting with three incoming XFEL pulses. The three laser frequencies and the relativistic factor γ of the accelerated nuclei are selected such that they Doppler shift the frequency of the x rays to match the target resonance. We show how to produce any desired superposition of two ground states in tripod nuclear systems by irradiating them with suitably chosen coherent light beams. This method is different from the proposed schemes in [13,14,22], where complete population transfer is investigated in three-level Λ-like nuclei systems. In the present scheme accelerated nuclei can interact with three XFEL laser beams in two frames. In the standard STIRAP frame, the nuclei interact by a time delay with the pump pulse compared to two other pulses; however, in the coincident pulses frame the nuclei interact with three laser beams without time delay. A fully coherent XFEL source, like the future XFEL oscillator XFELO [36] or the seeded XFEL (SXFEL) [1,37–41], was used for all laser pulses throughout the study. In order to calculate the necessary laser intensities for each technique we used the Morris-Shore transformation [42–44] and reduced the tripod system to a three-level Λ-like system. We selected ^{154}Gd, with a short lifetime excited state, and ^{97}Tc, with a long lifetime excited state, and the population can be transferred completely from the stable ground state to an arbitrary superposition of other ground states.

This paper is organized as follows. In Sec. II we describe briefly the coincident pulse and STIRAP techniques in tripod systems. The nuclear tripod linkage pattern and coherent superposition of states in this system are explained in Sec. III. In Sec. IV we present a numerical study of our method and demonstrate the effect of laser intensity fluctuation in the coincident pulse technique. The conclusions are summarized in Sec. V.

II. COINCIDENT PULSES AND STIRAP TECHNIQUES IN TRIPOD SYSTEMS

Figure 1(a) shows energy levels and linkage pattern of the tripod system. States $|1\rangle$ and $|4\rangle$ are coupled by the pulse with

*m.saadati@uma.ac.ir

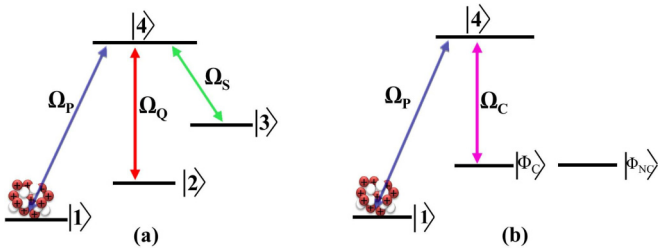

FIG. 1. (a) Linkage pattern of tripod system. All initial population is in state $|1\rangle$. (b) Linkage pattern of tripod system in Morris-Shore basis.

Rabi frequencies $\Omega_P(t)$, states $|2\rangle$ and $|4\rangle$ by the pulse with $\Omega_Q(t)$, and states $|3\rangle$ and $|4\rangle$ by the pulse with $\Omega_S(t)$. We assume that the Rabi frequencies are real and positive. The internal dynamics of the system is described by the time-dependent Schrödinger equation (TDSE),

$$i\hbar\frac{\partial}{\partial t}|\Psi(t)\rangle = \hat{H}(t)|\Psi(t)\rangle, \tag{1}$$

where $\hat{H}(t)$ is the Hamiltonian matrix in the subspace $S = \{|1\rangle,|2\rangle,|3\rangle,|4\rangle\}$ for the system and its interaction with the pulses. The state vector $|\Psi(t)\rangle$ is a four-component column vector. The Hamiltonian $\hat{H}(t)$ in the rotating-wave approximation [15,16] in exact resonance and in the absence of decoherence reads

$$\hat{H}(t) = \frac{\hbar}{2}\begin{pmatrix} 0 & 0 & 0 & \Omega_P(t) \\ 0 & 0 & 0 & \Omega_Q(t) \\ 0 & 0 & 0 & \Omega_S(t) \\ \Omega_P(t) & \Omega_Q(t) & \Omega_S(t) & 0 \end{pmatrix}. \tag{2}$$

We impose that the Rabi frequencies $\Omega_Q(t)$ and $\Omega_S(t)$ are pulse-shaped functions with the same time dependence, but possibly with different magnitudes. However, the Rabi frequency $\Omega_P(t)$ could have different magnitudes and time dependance than the others. We define the time-independent mixing angle θ such that $\tan\theta = \Omega_S(t)/\Omega_Q(t)$. Following the Morris-Shore (MS) transformation [42–44], one can find a constant unitary operator transforming the system into a coupled three-state Λ-like system and a noncoupled state. The transformed Hamiltonian in the MS basis $S_T = \{|1\rangle,|\phi_C\rangle,|4\rangle,|\phi_{NC}\rangle\}$ reduces to a three-state Λ-like system [25,26] [see Fig. 1(b)]:

$$\hat{H}_T(t) = \frac{\hbar}{2}\begin{pmatrix} 0 & 0 & \Omega_P(t) \\ 0 & 0 & \Omega_C(t) \\ \Omega_P(t) & \Omega_C(t) & 0 \end{pmatrix}, \tag{3}$$

where $\Omega_C(t) = \Omega_Q(t)/\cos\theta$ and the coupled state $|\phi_C\rangle = \cos\theta|2\rangle + \sin\theta|3\rangle$. Below we will explain how the coincident pulse and STIRAP techniques can be used for coherent superposition of states in nuclear tripod systems.

(a) Coincident pulses technique. In order to implement the coincident pulse technique in tripod systems, we impose that the Rabi frequencies $\Omega_P(t)$ and $\Omega_C(t)$ in Eq. (3) must be pulse-shaped functions with the same time dependence, but possibly with different magnitudes. Considering the bright-dark state [45,46], we use a sequence of coincident pulses, each with rms pulse area $A(t_f) = \int_{t_i}^{t_f}\sqrt{\Omega_{P_k}^2(t) + \Omega_{C_k}^2(t)}dt = 2\pi$ at the end of the kth step and mixing angles φ_k [23–27], with the following total evolution matrix:

$$\hat{U}^{(N)} = \hat{U}(\varphi_N)\hat{U}(\varphi_{N-1})\cdots\hat{U}(\varphi_k)\cdots\hat{U}(\varphi_1), \tag{4}$$

where

$$\tan\varphi_k = \frac{\Omega_{P_k}(t)}{\Omega_{C_k}(t)}. \tag{5}$$

According to the Ref. [23], φ_k must satisfy the following conditions:

(i) The population is transferred to state $|\phi_C\rangle$ (that corresponds to a coherent superposition of states $|2\rangle$ and $|3\rangle$) in the end; $P_{|1\rangle} = P_{|4\rangle} = 0$ and $P_{|\phi_C\rangle} = 1$.
(ii) The maximum of the transient population $P_{|4\rangle}(t)$ excited by each sequence of pulses $\Omega_{P_k}(t)$ and $\Omega_{C_k}(t)(\Omega_{Q_k}(t),\Omega_{S_k}(t))$ is the same.
(iii) The maximum population of state $|4\rangle$ in the middle of each sequence is damped to small values by increasing the number of pulse sets.

Considering the above conditions, the mixing angle φ_k is given by

$$\varphi_k = \frac{(2k-1)\pi}{4N} \quad (k = 1,2,3,\ldots,N). \tag{6}$$

Using this sequence of pulses, one can transfer the population of state $|1\rangle$ to $|\phi_C\rangle$ with a negligible population in state $|4\rangle$.

(b) STIRAP. In the subspace S_T, one of the eigenvalues of the Hamiltonian of Eq. (3) is zero. The corresponding eigenstate (dark state) of the Hamiltonian reads [17]

$$|D(t)\rangle = \frac{1}{\sqrt{\Omega_P^2(t) + \Omega_C^2(t)}}[\Omega_C(t)|1\rangle - \Omega_P(t)|\phi_C\rangle]. \tag{7}$$

The initial state of the system is $|1\rangle$. We initially turn on Rabi frequency $\Omega_C(t)(\Omega_Q(t),\Omega_S(t))$ while the first Rabi frequency $\Omega_P(t)$ is turned off. Then we adiabatically increase $\Omega_P(t)$ and decrease $\Omega_C(t)$ so that at the end of evolution the Rabi frequency $\Omega_C(t)$ is turned off and $\Omega_P(t)$ is turned on, and the system state evolves into the desired state $|\phi_C\rangle$.

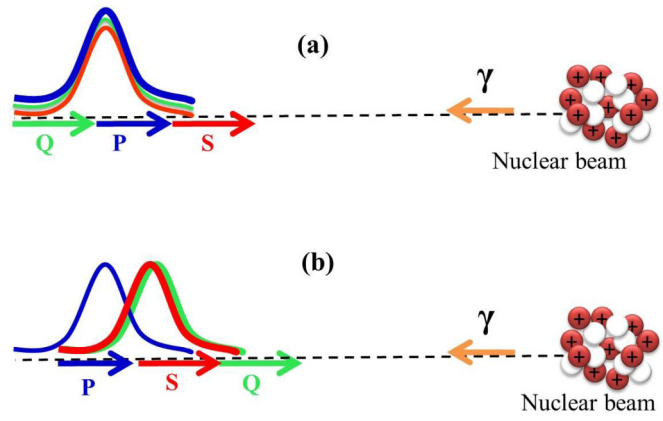

FIG. 2. (a) Coincident pulses and (b) STIRAP schemes in the laboratory frame. In both schemes each pulse has a different frequency from one another.

III. NUCLEAR TRIPOD SYSTEMS

We study the collider system depicted in Fig. 2, which is composed of an accelerated nuclear beam that interacts with three incoming XFEL pulses. In Fig. 2(a) all of the laser pulses are coincident, which corresponds to the coincident pulse technique. Also, in Fig. 2(b) the Rabi frequencies $\Omega_Q(t)$ and $\Omega_S(t)$ are coincident and have a delay time with $\Omega_P(t)$, which corresponds to the STIRAP technique. The three laser frequencies and the relativistic factor γ of the accelerated nuclei have to be chosen so that in the nuclear rest frame the condition of exact resonances is fulfilled. The nuclear dynamics is governed by the master equation for the nuclear density matrix $\hat{\rho}(t)$ [13,14,18,47]:

$$\frac{\partial}{\partial t}\hat{\rho} = \frac{1}{i\hbar}[\hat{H},\hat{\rho}] + \hat{\rho}_s + \hat{\rho}_d, \tag{8}$$

where the Hamiltonian $\hat{H}(t)$ is given by Eq. (2); $\hat{\rho}_s$ is the decoherence matrix caused by spontaneous emission from excited state $|4\rangle$ and unstable ground states ($|2\rangle$, $|3\rangle$). $\hat{\rho}_d$ is an additional dephasing matrix to model laser field pulses with limited coherence times. Taking into consideration the radioactive decays of states $|2\rangle$, $|3\rangle$, and $|4\rangle$ to the lower states of the linkage pattern, the decoherence matrix $\hat{\rho}_s$ is

$$\hat{\rho}_s = \begin{pmatrix} \Gamma_2 B_{21}\rho_{22} + \Gamma_3 B_{31}\rho_{33} + \Gamma_4 B_{41}\rho_{44} & -\frac{\Gamma_2}{2}\rho_{12} & -\frac{\Gamma_3}{2}\rho_{13} & -\frac{\Gamma_4}{2}\rho_{14} \\ -\frac{\Gamma_2}{2}\rho_{21} & -\Gamma_2\rho_{22} + \Gamma_3 B_{32}\rho_{33} + \Gamma_4 B_{42}\rho_{44} & -\frac{\Gamma_2+\Gamma_3}{2}\rho_{23} & -\frac{\Gamma_2+\Gamma_4}{2}\rho_{24} \\ -\frac{\Gamma_3}{2}\rho_{31} & -\frac{\Gamma_2+\Gamma_3}{2}\rho_{32} & -\Gamma_3\rho_{33} + \Gamma_4 B_{43}\rho_{44} & -\frac{\Gamma_3+\Gamma_4}{2}\rho_{34} \\ -\frac{\Gamma_4}{2}\rho_{41} & -\frac{\Gamma_2+\Gamma_4}{2}\rho_{42} & -\frac{\Gamma_3+\Gamma_4}{2}\rho_{43} & -\Gamma_4\rho_{44} \end{pmatrix}, \tag{9}$$

where Γ_k ($k = 2,3,4$) is the linewidth of state $|k\rangle$ and B_{ki} is the branching ratio of $|k\rangle \to |i\rangle$ ($i = 1,2,3$). The dephasing effect can be avoided by using a fully coherent XFEL to derive nuclear transitions. Considering a fully coherent XFEL source for all laser pulses, in our method the term $\hat{\rho}_d$ in Eq. (8) is zero. The Rabi frequencies can be obtained as follows [48–50]:

$$\Omega_{P(Q,S)}(t) = \frac{4\sqrt{\pi}}{\hbar}\left[\frac{\gamma^2(1+\beta)^2 I^{\rm eff}_{P(Q,S)}(L_{1(2,3)4}+1)(2I_{1(2,3)}+1)\mathbb{B}(\varepsilon/\mu L_{1(2,3)4})}{c\epsilon_0 L_{1(2,3)4}}\right]^{1/2} \times \frac{k_{41(2,3)}^{L_{1(2,3)4}-1}}{(2L_{1(2,3)4}+1)!!}\exp\left\{-\left[\frac{\gamma(1+\beta)(t-\tau_{P(Q,S)})}{\sqrt{2}T_{P(Q,S)}}\right]^2\right\}. \tag{10}$$

The above equation is an extension of the Rabi frequencies in Ref. [50] for an accelerated nucleus interacting with two x-ray $S(P)$ laser pulses. Here it is necessary to explain the concept of effective intensity $I^{\rm eff}_{P(Q,S)}$. For the long laser pulse case, the bandwidth of the incident laser of intensity $I_{P(Q,S)}$ is narrower than the linewidth Γ_4 of the considered nuclear transition [i.e., $\Gamma_4 \geqslant \gamma(1+\beta)\Gamma_{P(Q,S)}$], and as a result $I^{\rm eff}_{P(Q,S)} = I_{P(Q,S)}$. For the short pulse case the effective intensity is significantly reduced since the bandwidth of the incident laser is wider than Γ_4 [i.e., $\Gamma_4 < \gamma(1+\beta)\Gamma_{P(Q,S)}$], and the effective intensity $I^{\rm eff}_{P(Q,S)}$ can be obtained as follows:

$$I^{\rm eff}_{P(Q,S)} = I_{P(Q,S)}\frac{\Gamma_4}{\gamma(1+\beta)\Gamma_{P(Q,S)}}. \tag{11}$$

The explantation of the notations used throughout the following text and equations can be found in Table I. In the following we impose that $T_P = T_Q = T_S = T$.

A. Coincident pulses technique in nuclear tripod systems

In order to implement the coincident pulse technique in nuclear tripod systems, the Rabi frequencies for each nucleus (X) in the kth step can be rewritten in the following form:

$$\Omega_{P_kX}(t) = \Omega_{0PX}\sqrt{\zeta_P}\sin\varphi_k\exp\left\{-\left[\frac{(t-\tau)}{\tilde{T}}\right]^2\right\}, \tag{12a}$$

$$\Omega_{Q_kX}(t) = \chi_1\Omega_{0QX}\sqrt{\zeta_Q}\cos\varphi_k\exp\left\{-\left[\frac{(t-\tau)}{\tilde{T}}\right]^2\right\}, \tag{12b}$$

$$\Omega_{S_kX}(t) = \chi_2\Omega_{0SX}\sqrt{\zeta_S}\cos\varphi_k\exp\left\{-\left[\frac{(t-\tau)}{\tilde{T}}\right]^2\right\}, \tag{12c}$$

TABLE I. The notations used throughout the text. The indices $i = 1,2,3,4$ denote the four nuclear states showed in Fig. 1(a). The label Lab (Rest) indicates that the corresponding values are in the laboratory (nuclear rest) frame.

Parameters used for pulses		
Notation	Frame	Explanation
c	Any	Speed of light in vacuum
β	Lab	Velocity of the nuclear particle, in units of c
γ	Lab	Relativistic factor $\gamma = 1/\sqrt{1-\beta^2}$
k_{4i}	Rest	Wave number of $\|4\rangle \rightarrow \|i\rangle$ transition
$\Gamma_{LP(Q,S)}$	Lab	Laser bandwidth of $P(Q,S)$
$\tau_{P(Q,S)}$	Rest	Temporal peak position of laser pulses
$T_{P(Q,S)}$	Lab	Pulse duration of laser pulses
$I_{1(2,3)}$	Any	Angular momentum of ground state $\|1\rangle$ ($\|2\rangle$, $\|3\rangle$)
$L_{1(2,3)}$	Any	Multipolarity of the corresponding nuclear $\|i\rangle \rightarrow \|4\rangle$ transition
$I_{P(Q,S)}$	Lab	Peak intensity of laser pulses
$\mathbb{B}(\varepsilon/\mu L_{i4})$	Rest	Reduced transition probability for the nuclear electric (ε) or magnetic (μ) $\|i\rangle \rightarrow \|4\rangle$ transition

where τ is the time delay between two neighboring sets of coincident pulses and

$$\Omega_{0P(Q,S)X} = \frac{4\sqrt{\pi}k_{41(2,3)}^{L_{1(2,3)4}-1}}{\hbar(2L_{1(2,3)4}+1)!!}\left[\frac{\gamma^2(1+\beta)^2(L_{1(2,3)4}+1)(2I_{1(2,3)}+1)\mathbb{B}(\varepsilon/\mu L_{1(2,3)4})}{c\epsilon_0 L_{1(2,3)4}}\right]^{1/2}, \tag{13a}$$

$$\tilde{T} = \frac{\sqrt{2}T}{\gamma(1+\beta)}, \tag{13b}$$

$$\zeta_P = \frac{I_{P_k}^{\text{eff}}}{\sin^2\varphi_k}, \quad \zeta_Q = \frac{I_{Q_k}^{\text{eff}}}{\chi_1^2\cos^2\varphi_k}, \quad \zeta_S = \frac{I_{S_k}^{\text{eff}}}{\chi_2^2\cos^2\varphi_k}. \tag{13c}$$

The condition $A(t_f) = 2\pi$ at the end of each sequence of coincident pulses is satisfied if

$$\zeta_{P(Q,S)} = \left(\frac{2\sqrt{\pi}}{\tilde{T}\Omega_{0P(Q,S)X}}\right)^2. \tag{14}$$

Using Eqs. (11), (13), and (14) the real intensities in the laboratory frame for two different conditions can be written as follows:

(i) For $\Gamma_4 \geqslant \gamma(1+\beta)\Gamma_{P(Q,S)}$ we have

$$I_{P_k} = \left(\frac{2\sqrt{\pi}}{\tilde{T}\Omega_{0PX}}\right)^2 \sin^2\varphi_k,$$
$$I_{Q_k(S_k)} = \left(\frac{2\sqrt{\pi}}{\tilde{T}\Omega_{0Q(S)X}}\right)^2 \chi_{1(2)}^2\cos^2\varphi_k. \tag{15}$$

(ii) For $\Gamma_4 < \gamma(1+\beta)\Gamma_{P(Q,S)}$ we have

$$I_{P_k} = \left(\frac{2\sqrt{\pi}}{\tilde{T}\Omega_{0PX}}\right)^2 \frac{\gamma(1+\beta)\Gamma_{P(Q,S)}}{\Gamma_4}\sin^2\varphi_k,$$
$$I_{Q_k(S_k)} = \left(\frac{2\sqrt{\pi}}{\tilde{T}\Omega_{0Q(S)X}}\right)^2 \frac{\gamma(1+\beta)\Gamma_{P(Q,S)}}{\Gamma_4}\chi_{1(2)}^2\cos^2\varphi_k. \tag{16}$$

By adjusting the intensity of the laser pulses according to Eqs. (15) and (16), the population is transferred from initial state $|1\rangle$ to an arbitrary coherent superposition of desired states $|\phi_C\rangle = (\chi_1|2\rangle + \chi_2|3\rangle)$.

B. STIRAP technique in nuclear tripod systems

In this subsection we assume that the Rabi frequencies for each nucleus (X) can be rewritten in the following

TABLE II. Nuclear energy of state $|i\rangle$, E_i, with $i = 1,2,3,4$ (in keV), linewidth of state $|4\rangle$, the multipolarities, and reduced matrix elements (in Weisskopf units) for the transitions $|i\rangle \rightarrow |4\rangle$ with $i = 1,2,3$ are given.

Specification of nuclear levels						$\varepsilon/\mu L$			$\mathbb{B}(\varepsilon/\mu L)$ (W.u.)		
Nucleus	E_4 (keV)	E_3 (keV)	E_2 (keV)	E_1 (keV)	Linewidth of $\|4\rangle$ (meV)	L_{14}	L_{24}	L_{34}	$\|1\rangle \rightarrow \|4\rangle$	$\|2\rangle \rightarrow \|4\rangle$	$\|3\rangle \rightarrow \|4\rangle$
^{97}Tc	656.90	324.48	215.72	96.57	0.61	$E2$	$E1$	$E1$	5×10^{2}	7.2×10^{-5}	6.7×10^{-5}
^{154}Gd	1241.29	680.67	123.07	0.00	300	$E1$	$E1$	$E1$	4.4×10^{-2}	4.9×10^{-2}	5.7×10^{-3}

TABLE III. Branching ratio of $|4\rangle \to |i\rangle$ $(i = 1,2,3)$ and XFEL parameters. The accelerated nuclei have the relativistic factor γ, determined by the one-photon resonance condition $\gamma(1+\beta)\hbar\omega_P = ck_{41}$. $\hbar\omega_Q$ and $\hbar\omega_S$ denote the photon energies. The pump photon energy is 12.4 keV for SXFEL and 25 keV for XFELO.

Nucleus	Branching ratio			SXFEL			XFELO		
	B_{41}	B_{42}	B_{43}	γ	$\hbar\omega_Q$ (keV)	$\hbar\omega_S$ (keV)	γ	$\hbar\omega_Q$ (keV)	$\hbar\omega_S$ (keV)
^{97}Tc	0.9653	0.0058	0.0289	22.6	9.76	7.36	11.2	19.73	14.83
^{154}Gd	0.5167	0.4752	0.0026	50.1	11.17	5.59	24.8	22.52	11.31

form:

$$\Omega_{PX}(t) = \Omega_{0PX}\sqrt{\zeta'_P}\exp\left\{-\left[\frac{(t-\tau)}{\tilde{T}}\right]^2\right\}, \quad (17a)$$

$$\Omega_{QX}(t) = \chi_1\Omega_{0QX}\sqrt{\zeta'_Q}\exp\left\{-\left[\frac{(t+\tau)}{\tilde{T}}\right]^2\right\}, \quad (17b)$$

$$\Omega_{SX}(t) = \chi_2\Omega_{0SX}\sqrt{\zeta'_S}\exp\left\{-\left[\frac{(t+\tau)}{\tilde{T}}\right]^2\right\}, \quad (17c)$$

where 2τ is the time delay between laser pulses and

$$\zeta'_P = I_P^{\text{eff}}, \quad \zeta'_Q = \frac{I_Q^{\text{eff}}}{\chi_1^2}, \quad \zeta'_S = \frac{I_S^{\text{eff}}}{\chi_2^2}, \quad (18)$$

such that for superposition with equal amplitudes we have

$$\frac{\zeta'_Q}{\zeta'_S} = \left(\frac{\chi_2\Omega_{0SX}}{\chi_1\Omega_{0QX}}\right)^2. \quad (19)$$

.

In order to satisfy the condition of adiabaticity for STIRAP, the laser intensities should be sufficiently large [18], and the relation between the real intensities in the laboratory frame and the effective laser intensities for two different conditions can be written as follows:

(i) For $\Gamma_4 \geqslant \gamma(1+\beta)\Gamma_{P(Q,S)}$ we have

$$I_{P(Q,S)} = I_{P(Q,S)}^{\text{eff}}. \quad (20)$$

(ii) For $\Gamma_4 < \gamma(1+\beta)\Gamma_{P(Q,S)}$ using (11) the real intensities in the laboratory frame can be calculated. By satisfying the above conditions one can create an arbitrary coherent superposition of states $(|\phi_C\rangle = (\chi_1|2\rangle + \chi_2|3\rangle))$ using the STIRAP technique in nuclear systems.

IV. NUMERICAL STUDY

For the numerical study, we choose ^{154}Gd and ^{97}Tc. We consider for both schemes that the pulse duration and bandwith of the SXFEL laser pulse are $T_{P(Q,S)} = 0.1$ ps and $\Gamma_{P(Q,S)} = 10$ meV [38]. Tables II and III represent the essential parameters for the numerical study. In Figs. 3 and 4 we clearly see the working conditions for STIRAP and coincident pulse

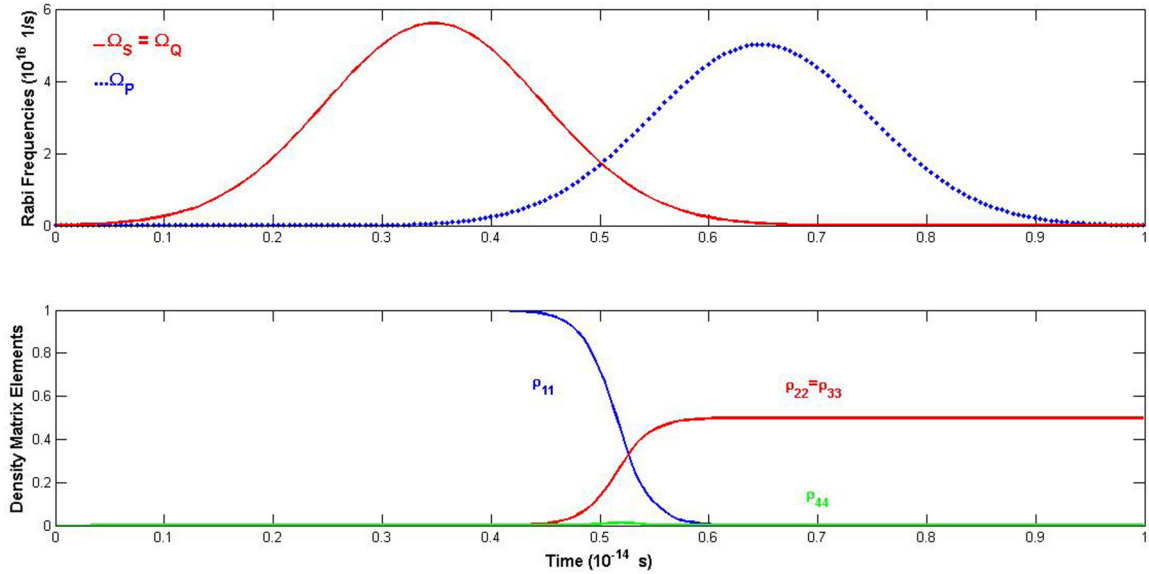

FIG. 3. Rabi frequencies in the nuclear rest frame (top frame) and diagonal elements of density matrix ρ_{mm} $(m = 1,2,3,4)$ in accordance with the populations of states $|1\rangle$, $|2\rangle$, $|3\rangle$, and $|4\rangle$ (lower frame) vs time for ^{154}Gd in the STIRAP frame using SXFEL parameters in master equation (8). The population of the state $|4\rangle$ is zero during the whole dynamics. The linewidths and branching ratios of states $|3\rangle$ and $|2\rangle$ are $\Gamma_3 = 102 \times 10^{-3}$ meV, $\Gamma_2 = 393 \times 10^{-6}$ meV, $B_{32} = 1$, $B_{31} = 0$, and $B_{21} = 1$. The real intensities of XFEL pulses are $I_p = 26.34 \times 10^{23}$ W/cm^2, $I_Q = 9.46 \times 10^{22}$ W/cm^2, and $I_S = 40.66 \times 10^{23}$ W/cm^2; $\tau = 1.5 \times 10^{-15}$ s. See the discussion in the text and Tables II and III for further parameters.

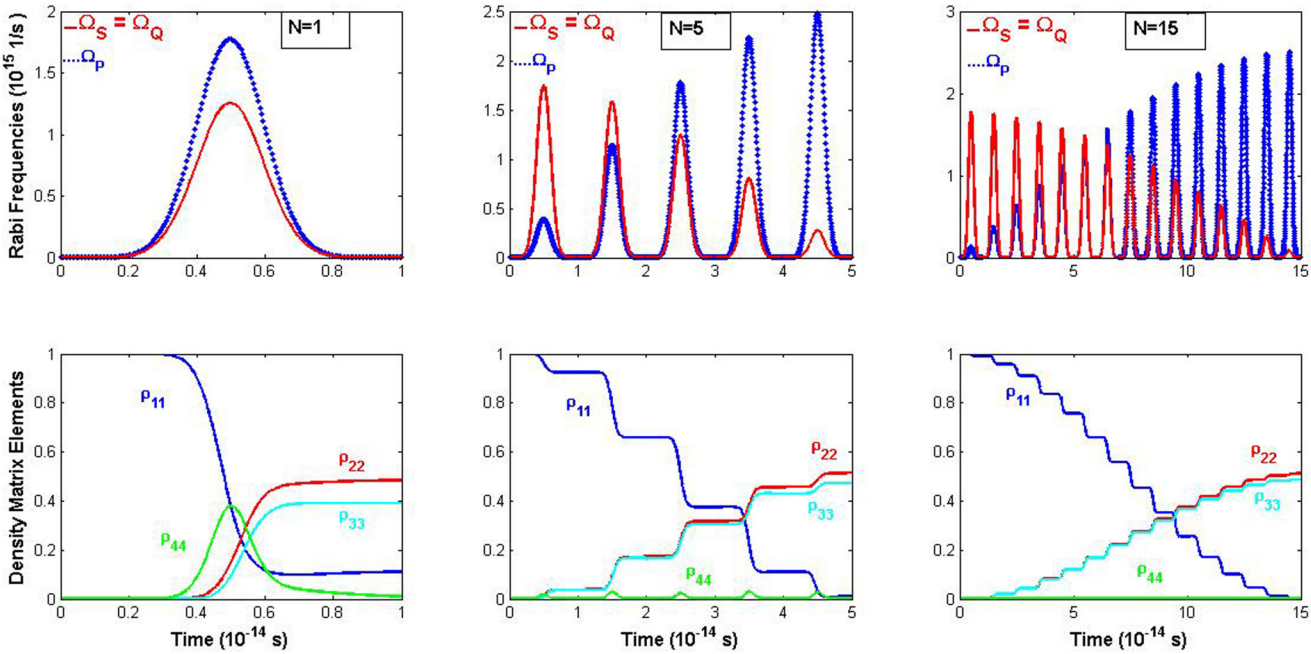

FIG. 4. Rabi frequencies in the nuclear rest frame (first row) and diagonal elements of density matrix ρ_{mm} ($m = 1,2,3,4$) in accordance with the populations of states $|1\rangle$, $|2\rangle$, $|3\rangle$, and $|4\rangle$ (second row) vs time for ^{154}Gd in the coincident pulse frame using SXFEL parameters in master equation (8). The linewidth and branching ratioes of states $|3\rangle$ and $|2\rangle$ are $\Gamma_3 = 102 \times 10^{-3}$ meV, $\Gamma_2 = 393 \times 10^{-6}$ meV, $B_{32} = 1$, $B_{31} = 0$, and $B_{21} = 1$. The real intensities of XFEL pulses in the kth step are $I_{P_k} = 26.338 \times 10^{19} \sin^2 \varphi_k$ W/cm^2, $I_{Q_k} = 2.37 \times 10^{19} \cos^2 \varphi_k$ W/cm^2, and $I_{S_k} = 10.17 \times 10^{20} \cos^2 \varphi_k$ W/cm^2. See the discussion in the text and Tables II and III for further parameters.

techniques using SXFEL pulses in ^{154}Gd, which correspond to the superposition of states $|2\rangle$ and $|3\rangle$ with equal amplitudes. In ^{154}Gd the lifetime of excited state $|4\rangle$ is 1.54 fs which is similar to the laser pulse duration in the nuclear rest frame. As can be expected, complete population transfer occurs using STIRAP. However, it needs a train of coincident pulses to complete population transfer in ^{154}Gd (see Fig 4). STIRAP needs large laser pulses intensities compared to the coincident pulse technique, which may be hard to reach experimentally. The other nucleus which can be used as a tripod system is ^{97}Tc, in which the lifetime of excited state $|4\rangle$ is 0.76 ps, which is longer than the XFEL pulse duration in the nuclear rest frame. Coherent superposition of states $|2\rangle$ and $|3\rangle$ with equal amplitudes can be achieved using SXFEL pulses in

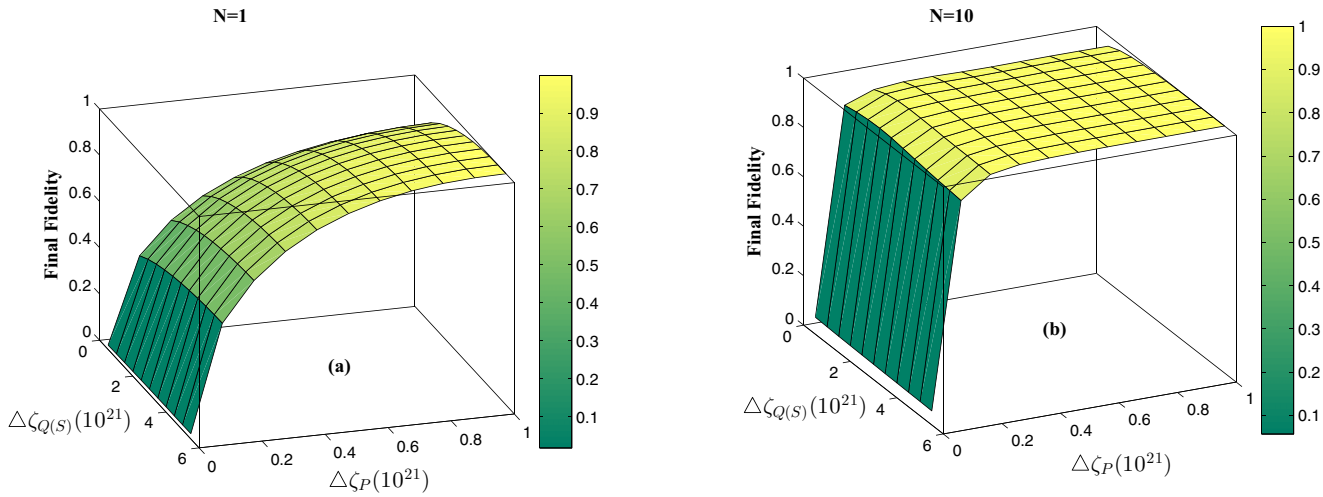

FIG. 5. Final fidelity of desired state $\frac{1}{\sqrt{2}}(|2\rangle + |3\rangle)$ as a function of $\Delta\zeta_P, \Delta(\zeta_{Q(S)})$ so that $\zeta_P = (0.0002 + \Delta\zeta_P) \times 10^{21}$ W/cm^2, $\zeta_Q = (1.0293 + \Delta(\zeta_Q)) \times 10^{21}$ W/cm^2, and $\zeta_S = (6.757 + \Delta(\zeta_S)) \times 10^{21}$ W/cm^2 for ^{97}Tc by using SXFEL parameters for $N = 1$ (a) and $N = 10$ (b) sequences of coincident pulses (in this case we consider the radioactive decay of state $|4\rangle$). The highest values of the horizontal axis lead to calculated real intensities in the kth step of $I_{P_k} = 740.76 \times 10^{21} \sin^2 \varphi_k$ W/cm^2, $I_{Q_k} = 223.27 \times 10^{22} \cos^2 \varphi_k$ W/cm^2, and $I_{S_k} = 435.37 \times 10^{22} \cos^2 \varphi_k$ W/cm^2. See the discussion in the text and Tables II and III for further parameters.

TABLE IV. The final populations of states $|2\rangle$ and $|3\rangle$ without and with taking into account the radioactive decay of states $|3\rangle$ to $|2\rangle, |1\rangle$ and $|2\rangle$ to $|1\rangle$. All parameters are the same as in Figs. 3 and 4.

Technique	Populations without the decay of states $\|3\rangle$ and $\|2\rangle$		Populations with the decay of states $\|3\rangle$ and $\|2\rangle$	
	Final population of $\|2\rangle$	Final population of $\|3\rangle$	Final population of $\|2\rangle$	Final population of $\|3\rangle$
STIRAP	0.5004	0.4987	0.5007	0.4985
Coincident pulse				
$N = 1$	0.4849	0.3919	0.4852	0.3916
$N = 5$	0.5127	0.4753	0.5146	0.4732
$N = 15$	0.5060	0.4922	0.5122	0.4859

^{97}Tc for $I_{P_k} = 740.76 \times 10^{21} \sin^2 \varphi_k$ W/cm^2, $I_{Q_k} = 223.27 \times 10^{22} \cos^2 \varphi_k$ W/cm^2, and $I_{S_k} = 435.37 \times 10^{22} \cos^2 \varphi_k$ W/cm^2 in the kth sequence of the coincident pulse technique. In order to implement the STIRAP technique in ^{97}Tc, we can use $I_p = 740.76 \times 10^{23}$ W/cm^2, $I_Q = 225.60 \times 10^{24}$ W/cm^2, and $I_S = 435.37 \times 10^{24}$ W/cm^2.

One issue that needs to be addressed in more detail is the role of laser intensity fluctuations on population transfer efficiency. STIRAP is robust against small variations of laser intensity. However nuclear state superposition by one sequence of coincident pulses needs precise adjustment of laser intensities. We plot in Fig. 5 results for ^{97}Tc using SXFEL to show the influence of the deviation of the laser intensities on the final fidelity of the desired state $[|\psi_d\rangle = \frac{1}{\sqrt{2}}(|2\rangle + |3\rangle)]$, which is defined as $F = |\langle\psi_d|\psi(t_f)\rangle|^2$. One can notice that the robustness of system to deviation from the calculated quantities in the kth step (i.e., $I_{P_k} = 740.76 \times 10^{21} \sin^2 \varphi_k$ W/cm^2, $I_{Q_k} = 223.27 \times 10^{22} \cos^2 \varphi_k$ W/cm^2, and $I_{S_k} = 435.37 \times 10^{22} \cos^2 \varphi_k$ W/cm^2) increases by increasing the number of coincident pulses from $N = 1$ [Fig. 5(a)] to $N = 10$ [Fig. 5(b)].

In the numerical studies of Figs. 3 and 4 we considered radioactive decays of excited state $|4\rangle$ and other unstable ground states $|2\rangle$ and $|3\rangle$. The lifetime of states $|2\rangle$ and $|3\rangle$ in ^{154}Gd is longer than the laser pulse duration in the nuclear rest frame, and the populations of states $|2\rangle$ and $|3\rangle$ do not significantly affect the efficiency of coherent superposition of states $|2\rangle$ and $|3\rangle$ with equal amplitudes. We present in Table IV the final populations of states $|2\rangle$ and $|3\rangle$ without and with radioactive decays of these states with the same intensities.

V. DISCUSSION AND CONCLUSION

In summary, we have investigated coherent superposition of states in nuclear tripod systems using coincident pulses and STIRAP techniques. Using these schemes, one can create a nuclear coherent superposition of states with relatively low energy hard x-ray photons. The required intensities of the three laser pulses used were derived to create coherent superposition of two unstable ground states from a single ground state in ^{154}Gd and ^{97}Tc. In the STIRAP technique we selected the laser intensities to be sufficiently large to satisfy the condition of adiabaticity for STIRAP.

The proposed method in this paper has some advantages in experimental implementations. In both techniques, we used a copropagating laser beam setup in which the number of the coherently excited nuclei is significant and has a better chance to be realized experimentally in the near future [14]. In the coincident pulse technique, we have shown that the robustness of the system to deviation from the calculated intensities increases by increasing the number of pulse sets. Besides that, after each sequence of pulses the populations of the system are in three ground states, and as a result the time delays between the neighboring pulses will not affect population transfer efficiency.

Coherent excitation of nuclear states can be used in coherent γ-ray spectroscopy. Traditional γ-ray spectroscopy measures only total intensity, which is proportional to diagonal elements of the density matrix. Coherent γ-ray spectroscopy gives additional information that can be used for the optical measurement of nuclear properties. The superpositions of states in our method are not degenerate. So there will be a clock-like reference phase that will be running with them. Very high frequency, so possibly an extremely precise clock might result. Also, coherent superposition of states can be used for quantum-beat spectroscopy in nuclear systems, which represents a beautiful demonstration of the fundamental principles of quantum mechanics. The quantum beat occurs as a result of coherent superposition of nondegenerate states $|2\rangle$ and $|3\rangle$ excited from lower level $|1\rangle$. The interference of the time dependent wave functions of the two coherently excited levels leads to this phenomenon [51].

ACKNOWLEDGMENT

We wish to acknowledge the financial support of the University of Mohaghegh Ardabili.

[1] M. Altarelli *et al.*, *XFEL: The European X-Ray Free-Electron Laser. Technical Design Report* (DESY, Hamburg, 2009).
[2] T. J. Bürvenich, J. Evers, and C. H. Keitel, Phys. Rev. Lett. **96**, 142501 (2006).
[3] A. Pálffy, J. Mod. Opt. **55**, 2603 (2008).
[4] I. Wong, A. Grigoriu, J. Roslund, T.-S. Ho, and H. Rabitz, Phys. Rev. A **84**, 053429 (2011).
[5] A. Junker, A. Pálffy, and C. H. Keitel, New J. Phys. **14**, 085025 (2012).

[6] B. Adams, C. Buth, S. M. Cavaletto, J. Evers, Z. Harman, C. H. Keitel, A. Pálffy, A. Picón, R. Röhlsberger, Y. Rostovtsev *et al.*, J. Mod. Opt. **60**, 2 (2013).

[7] J. Gunst, Y. A. Litvinov, C. H. Keitel, and A. Pálffy, Phys. Rev. Lett. **112**, 082501 (2014).

[8] X. Kong, W.-T. Liao, and A. Pálffy, New J. Phys. **16**, 013049 (2014).

[9] W.-T. Liao and A. Pálffy, Phys. Rev. Lett. **112**, 057401 (2014).

[10] A. Pálffy, Nat. Phys. **11**, 893 (2015).

[11] X. Kong and A. Pálffy, Phys. Rev. Lett. **116**, 197402 (2016).

[12] J. Gunst, C. H. Keitel, and A. Pálffy, Sci. Rep. **6**, 25136 (2016).

[13] W.-T. Liao, A. Pálffy, and C. H. Keitel, Phys. Lett. B. **705**, 134 (2011).

[14] W.-T. Liao, A. Pálffy, and C. H. Keitel, Phys. Rev. C. **87**, 054609 (2013).

[15] L. Allen and J. H. Eberly, *Optical Resonance and Two-Level Atoms* (Wiley, New York, 1975).

[16] B. W. Shore, *The Theory of Coherent Atomic Excitation* (Wiley, New York, 1990).

[17] U. Gaubatz, P. Rudecki, S. Schiemann, and K. Bergmann, J. Chem. Phys. **92**, 5363 (1990).

[18] K. Bergmann, H. Theuer, and B. W. Shore, Rev. Mod. Phys. **70**, 1003 (1998).

[19] N. V. Vitanov, M. Fleischhauer, B. W. Shore, and K. Bergmann, Adv. At. Mol. Opt. Phys. **46**, 55 (2001).

[20] N. V. Vitanov, T. Halfmann, B. W. Shore, and K. Bergmann, Annu. Rev. Phys. Chem. **52**, 763 (2001).

[21] K. Bergmann, N. V. Vitanov, and B. W. Shore, J. Chem. Phys. **142**, 170901 (2015).

[22] B. Nedaee-Shakarab, M. Saadati-Niari, and F. Zolfagharpour, Phys. Rev. C **94**, 054601 (2016).

[23] A. A. Rangelov and N. V. Vitanov, Phys. Rev. A **85**, 043407 (2012).

[24] M. Amniat-Talab and M. Saadati-Niari, J. Mod. Opt. **61**, 877 (2014).

[25] M. Saadati-Niari and M. Amniat-Talab, J. Mod. Opt. **61**, 1492 (2014).

[26] M. Amniat-Talab and M. Saadati-Niari, Eur. Phys. J. D. **69**, 215 (2015).

[27] M. Saadati-Niari, Ann. Phys. **372**, 138 (2016).

[28] E. A. Shapiro, V. Milner, C. Menzel-Jones, and M. Shapiro, Phys. Rev. Lett. **99**, 033002 (2007).

[29] S. Zhdanovich, E. A. Shapiro, M. Shapiro, J. W. Hepburn, and V. Milner, Phys. Rev. Lett. **100**, 103004 (2008).

[30] E. A. Shapiro, A. Peer, J. Ye, and M. Shapiro, Phys. Rev. Lett. **101**, 023601 (2008).

[31] R. G. Unanyan, M. Fleischhauer, B. W. Shore, and K. Bergmann, Opt. Commun. **155**, 144 (1998).

[32] Z. Kis and F. Renzoni, Phys. Rev. A. **65**, 032318 (2002).

[33] E. S. Kyoseva and N. V. Vitanov, Phys. Rev. A **73**, 023420 (2006).

[34] M. Amniat-Talab, M. Saadati-Niari, S. Guerin, and R. Nader-Ali, Phys. Rev. A **83**, 013817 (2011).

[35] M. Amniat-Talab, M. Saadati-Niari, and S. Guérin, Eur. Phys. J. D **66**, 216 (2012).

[36] K.-J. Kim, Y. Shvyd'ko, and S. Reiche, Phys. Rev. Lett. **100**, 244802 (2008).

[37] J. Feldhaus, E. L. Saldin, J. R. Schneider, E. A. Schneidmiller, and M. V. Yurkov, Opt. Commun. **140**, 341 (1997).

[38] E. L. Saldin, E. A. Schneidmiller, Y. V. Shvyd'ko, and M. V. Yurkov, Nucl. Instrum. Methods A **475**, 357 (2001).

[39] J. Arthur *et al.*, *Linac Coherent Light Source (LCLS), Conceptual Design Report* (SLAC, Stanford, CA, 2002).

[40] M. Yabashi and T. Ishikawa, *XFEL/SPring-8 Beamline Technical Design Report Ver. 2.0* (RIKEN-JASRI, Harima, Japan, 2010).

[41] J. Stohr *et al.*, Linac Coherent Light Source II Conceptual Design Report, 2011, https://portal.slac.stanford.edu/sites/lcls_public/lcls_ii/Pages/default.aspx

[42] J. R. Morris and B. W. Shore, Phys. Rev. A. **27**, 906 (1983).

[43] A. A. Rangelov, N. V. Vitanov, and B. W. Shore, Phys. Rev. A. **74**, 053402 (2006).

[44] B. W. Shore, J. Mod. Opt. **61**, 787 (2014).

[45] D. P. Pegg and W. R. Macgillivary, Opt. Commun. **59**, 113 (1986).

[46] N. V. Vitanov, J. Phys. B. **31**, 709 (1998).

[47] M. O. Scully, E. S. Fry, C. H. R. Ooi, and K. Wódkiewicz, Phys. Rev. Lett. **96**, 010501 (2006).

[48] J. M. Blatt and V. F. Weisskopf, *Theoretical Nuclear Physics* (Dover, Mineola, NY, 1991).

[49] A. Pálffy, J. Evers, and C. H. Keitel, Phys. Rev. C. **77**, 044602 (2008).

[50] W. T. Liao, *Coherent Control of Nuclei and X-Rays* (Springer, Berlin, 2013).

[51] W. Demtröder, *Laser Spectroscopy: Basic Concepts and Instrumention* (Springer, Berlin, 2013).